Modeling Finger Number Dependence on RF Noise to 10 GHz in 0.13μm Node MOSFETs with 80nm Gate Length

M.C. King[1], Z. M. Lai[1], C. H. Huang[1,3], C. F. Lee[1], M. W. Ma[1], C. M. Huang[2], Yun Chang[2] and Albert Chin[1]

[1] Dept. of Electronics Eng., National Chiao Tung Univ., Hsinchu, Taiwan
[2] Taiwan Semiconductor Manufacturing Corp., Science-Based Industrial Park, Tainan 741-44, Taiwan
[3] Currently at Taiwan Semiconductor Manufacturing Corp., Science-Based Industrial Park, Hsinchu, Taiwan

***Abstract* — We have modeled the as-measured and de-embedded NF_{min} on multi-fingers 0.13 μm node MOSFETs. In contrast to the as-measured large NF_{min} value and strong dependence on parallel gate fingers, the de-embedded NF_{min} has much smaller noise of only 1.1-1.2 dB for 6, 18 and 36 fingers and weak dependence. From the well calibrated equivalent circuit model with as-measured NF_{min}, the dominant noise source is from the probing pad generated thermal noise. From our derived equation with excellent agreement with de-embedded NF_{min} to 10 GHz, the weak dependence of intrinsic NF_{min} on gate finger is due to the combined effect of $R_g g_m$ and drain hot carrier noise but both have weak dependence on finger numbers.**

I. INTRODUCTION

The increasing operation frequency to higher band with wider bandwidth is the technology trend for communication system. The demand of high performance low noise MOSFET becomes more urgent for ultra-wide band (UWB) (3.1-10.6 GHz) beyond current W-LAN (5.2-5.8 GHz), since the noise also increases monotonically with increasing frequency. However, accurate RF noise modeling of the nm-scale MOSFETs is challenging due to the limited understanding of noise sources and the large parasitic effect from low resistivity Si substrate [1]-[3]. Another problem for the nm-scale MOSFET is the large gate resistance where a parallel multiple gate fingers layout is used to reduce the R_g generated thermal noise [3]. Unfortunately, the consumed DC and RF power also increase with increasing finger number that is contradictory to the low power trend. In this paper, we have modeled and analyzed the minimum noise figure (NF_{min}) of multi-fingers 0.13μm node MOSFETs (~80 nm physical gate length) using low-voltage logic process. In contrast to the as-measured large NF_{min} value and strong dependence on parallel fingers, the de-embedded intrinsic NF_{min} has much smaller noise value and weak dependence on gate fingers. From measured data and circuit analysis, the large as-measured NF_{min} is due to the small impedance of large probing (substrate loss) that dominating the measured noise [3]. We have derived an analytical equation to analyze the weak dependence of de-embedded NF_{min} on gate finger, which has exactly the same dependence of f, C_{gs} and g_m with Fukui's experimental equation [4] for GaAs FETs and fits well the de-embedded NF_{min} over the whole frequency range to 10 GHz. The weak finger width dependence is explained by the combined effect of $R_g g_m$ and drain hot carrier noise [5] in short channel devices that have small dependence on finger number. Therefore, good DC and RF integrity of very low noise of 1.1 dB at 10 GHz, low current consumption of 11 mA and high f_T of 125 GHz can be simultaneously obtained in the de-embedded 80nm MOSFETs with the smallest 6 fingers.

II. EXPERIMENTAL PROCEDURE

Multiple gate-fingers layout is used to reduce the gate resistance (8 Ω/sq) of 0.13 μm node MOSFETs (L_G ~80 nm) by connecting them in parallel. Large gate fingers from 6, 18 to 36 are studied but the drain current also increases from 11, 28 to 57 mA. Further increasing gate finger beyond 36 is limited by the large power consumption. The S-parameters are measured from 300 MHz to 30 GHz using network analyzer. The NF_{min} and associated gain are measured using ATN-NP5B Noise Parameter Extraction System up to 10 GHz and useful for UWB. The conventional way to de-embed NF_{min} requires removing parasitic open and through lines effects from as-measured NF_{min} by using series matrix calculations [6]. In this work, we have used the same ideal but the equivalent circuit model to de-embed the measured NF_{min}. This method can give not only the de-embedded NF_{min} but also additional information of noise source analysis beyond conventional method. As shown in Fig. 1, the un-de-embedded noise model includes the MOSFET, through lines [1]-[2] and probing pads at both I/O ports. The BSIM3 model parameters of MOSFET in Fig. 1 are obtained by standard extraction procedure. To reduce the through line effect, the layout of very short and thin transmission line, shown in Fig. 2, is used to largely

0-7803-8333-8/04/$20.00 © 2004 IEEE

reduce the thermal noise from series R_{thru} and shunt R_{sub} of through line. This is justified from the contributed DC resistance of only ~0.2 Ω from the through line and also proven by the Electro-Magnetic Simulation [2].

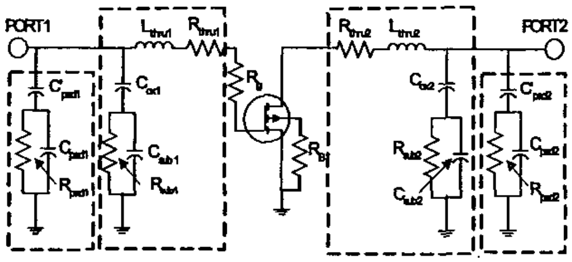

Fig. 1. The extrinsic equivalent circuit model for RF MOSFET that contains intrinsic BSIM3 MOSFET model, connected gate resistance R_g, through transmission lines and probing pads. The shunt impedance to ground from through line is much larger than probing pad due to the short and thin line layout.

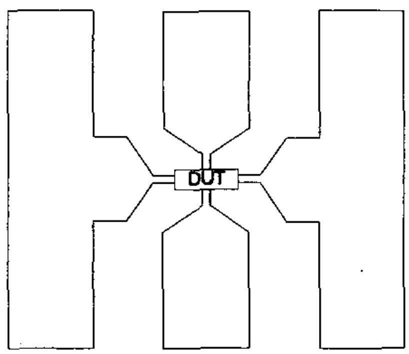

Fig. 2. The schematic diagram of probing pad and through transmission line connected to device under test. Short and thin through line is used to reduce its noise generation.

III. RESULTS AND DISCUSSION

A. De-embedded noise from measured NF_{min} and S:

Since the measured noise includes the large probing pad effect, we have first simulated the as-measured S-parameters with pad. Figs. 3(a) and 3(b) show the as-measured and modeled S-parameters for the smallest 6 and largest 36 fingers 80nm MOSFETs, respectively. Good agreement between measured and modeled S-parameters is obtained suggesting the good accuracy of circuit model in Fig. 1, where the equivalent circuit model for open pad in I/O ports is from the well matched simulation of open pad sub-circuit with measured S-parameters.

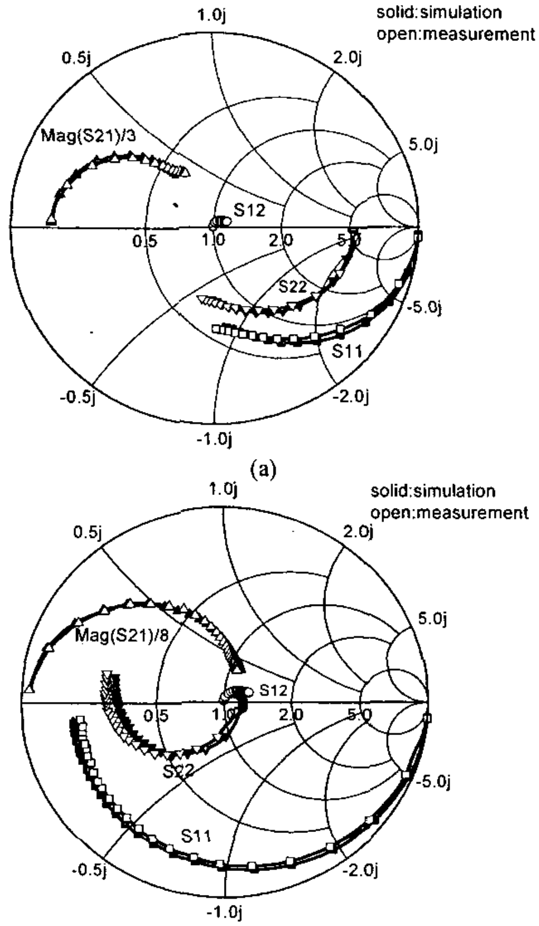

Fig. 3. The as-measured and modeled S-parameters of 80 nm MOSFETs with probing pad for (a) the smallest 6 and (b) the largest 36 gate fingers. The good agreement indicates the good accuracy of model in Fig. 1. The S_{21} is divided by respective 3 or 8 to fit in the unity radius Smith Chart due to the large gain.

Figs. 4(a) and 4(b) show the as-measured and simulated NF_{min} of the smallest 6 and largest 36 fingers 80nm MOSFETs, respectively, where the simulated data is from the equivalent circuit model in Fig. 1 with extrinsic modeling parameters from the well matched S-parameters in Fig. 3. The excellent agreement between as-measured and simulated NF_{min}, in combining with the well matched S-parameters in Fig. 3, indicates the good accuracy of circuit model in Fig. 1. Similar good agreement is also obtained for the 18 fingers MOSFETs (not shown). Therefore, the same model is suitable to provide self-consistent solutions for NF_{min}, S-parameters, and DC (from extracted BSIM3 modeling parameters).

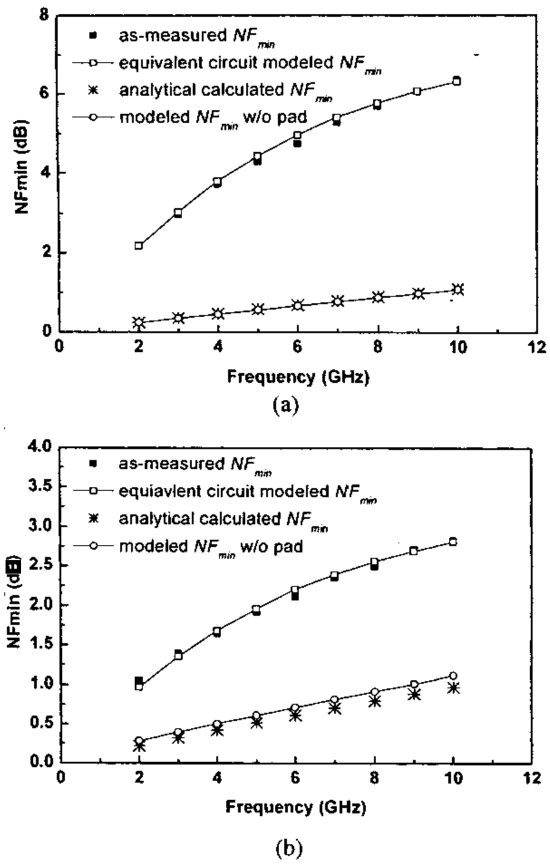

Fig. 4. The measured and modeled NF_{min} of 80 nm MOSFETs with (a) the smallest 6 and (b) the largest 36 fingers. The good agreement between as-measured and simulated NF_{min} indicates the good accuracy of model in Fig. 1. The probing pad shows the dominant effect on as-measured NF_{min}. The analytical calculation is also added from derived equation (4) for comparison.

We have further used the well matched equivalent circuit model to de-embed the noise generated from the probing pad. The pad equivalent sub-circuit is included inside the extrinsic model in Fig. 1 and the parameters values are obtained from the well agreed simulation data with measured S-parameters of open pad. The de-embedded NF_{min} is also shown in Fig. 4, which is largely reduced from as-measured data to only 1.1-1.2 dB at 10 GHz for both fingers MOSFETs. Similar largely reduced NF_{min} to 1.1 dB is also obtained for 18 fingers case (not shown). This suggests that the probing pad contributes the dominant noise source in as-measured NF_{min} because of its low impedance shunt pass connected to gate [3], where such effect can be greatly reduced by increasing substrate resistivity [1]-[2].

B. *Analysis of de-embedded NF_{min}:*

To further understand such large contribution of probing pad, we have analyzed the excess noise generated by both pad and gate resistance. Fig. 5(a) shows the typical noise circuit of MOSFETs with two equivalent input noise generators [5]. However, this simplified noise circuit did not consider the thermal noise from both gate resistance and shunt pass resistance of probing pad. Fig. 5(b) shows the modified noise circuit including the R_g and R_{pad} thermal noise sources. To include these additional thermal noises and translate into the two equivalent input noise generators in Fig. 4(a), short and open circuiting the input are required. The reason why open pad R_{pad} generates dominant noise is due to the formation series or parallel connection with R_g during open or short circuiting. Since the R_{pad} is larger than R_g even at the smallest 6 finger devices, its generated thermal noise becomes the dominant factor in NF_{min}.

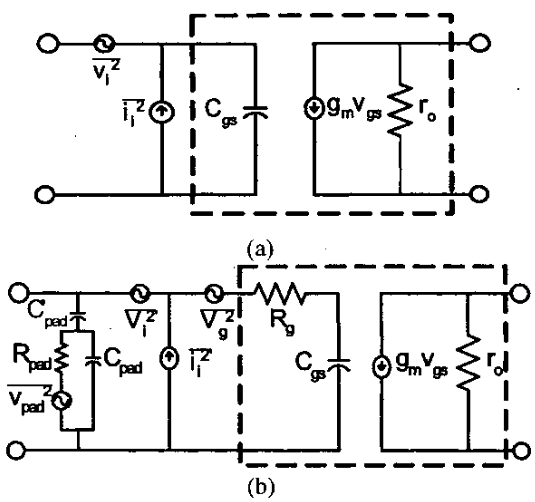

Fig. 5. The noise circuit of MOSFETs with (a) simplified two equivalent input noise generators and (b) our proposed model with additional noises from R_g and R_{pad}. To convert our proposed noise circuit in (b) into two equivalent input noise generators case in (a), open and short circuiting are required.

To analyze the reason why the de-embed NF_{min} having only weak finger number dependence, we have derived the NF_{min} based on the intrinsic equivalent MOSFET circuit in Fig. 1 with additional R_g and following the procedure in reference [5]:

$$\frac{\overline{v_i^2}}{\Delta f} = 4kT\gamma\frac{1}{g_m} + \frac{K_f}{WLC_{OX}f} + 4kTR_g \cong 4kT\left(\frac{\gamma}{g_m} + R_g\right) \quad (1)$$

$$\frac{\overline{i_i^2}}{\Delta f} = 2qI_G + \frac{\omega^2 C_{gs}^2}{g_m^2}\left(4kT\gamma g_m + K\frac{I_D}{f}\right) \cong 4kT\omega^2 C_{gs}^2 \frac{\gamma}{g_m} \quad (2)$$

$$NF = 1 + \frac{\overline{v_i^2}}{4kTR_S\Delta f} + \frac{\overline{i_i^2}}{4kT\frac{1}{R_s}\Delta f} \approx 1 + \frac{1}{R_S}\left(\frac{\gamma}{g_m} + R_g\right) + R_s\omega^2 C_{gs}^2\left(\frac{\gamma}{g_m}\right) \quad (3)$$

$$NF_{min} \approx 1 + 4\pi f\frac{C_{gs}}{g_m}\sqrt{\gamma^2 + \gamma\cdot g_m R_g} = 1 + 2\gamma\frac{f}{f_t}\sqrt{\gamma + g_m R_g} \quad (4)$$

In above equations, the $1/f$ terms are neglected due to high RF frequency. The γ is the proportional constant of the drain current noise, which was previously attributed to hot electron effect in short channels. The derived NF_{min} in equation (4) has exactly the same dependence of f, C_{gs} and g_m with Fukui's experimental equation [4] for GaAs FETs that suggests the good accuracy of the derived equation. This is further evidenced from the close agreement with the de-embedded NF_{min} plotted in Figs. 4(a) and 4(b) over the whole frequency range of 2-10 GHz. The γ value of 1.3-1.7 for 6, 18 (not shown) and 36 fingers 80nm MOSFETs also agrees well with the published data of short gate length MOSFETs [5]. Since the increasing parallel gate fingers will reduce the R_g but also increase the g_m, the $R_g g_m$ and γ all give nearly constant value regardless the number of fingers. The weak dependence of de-embedded NF_{min} with finger number may come from the measured slightly decreasing f_t with increasing finger number due to the increasing C_{gd} and parasitic capacitance. This result suggests that small fingers MOSFET can be used for LNA design and achieve low power consumption at the same time.

IV. CONCLUSION

We have shown that the dominant noise source is from the probing pad generated thermal noise, which is due to the lossy Si substrate effect. The NF_{min} is largely reduced from the as-measured 3-6 dB to only small 1.1-1.2 dB after de-embedding for 6, 18 and 36 fingers 80nm MOSFETs. The weak dependence of NF_{min} after de-embedding is due to the combined effect of $R_g g_m$ and nearly constant γ where the increasing finger number decreases R_g but also increases g_m monotonically.

ACKNOWLEDGEMENT

The authors wish to acknowledge the assistance and support of all the researchers in Prof. Chin's Microwave Lab and M. T. Yang, C. W. Kuo, and C. T. Lin in tsmc.

REFERENCES

[1]. K. T. Chan, A. Chin, S. P. McAlister, C. Y. Chang, V. Liang, J. K. Chen, S. C. Chien, D. S. Duh, and W. J. Lin, "Low RF loss and noise of transmission lines on Si substrates using an improved ion implantation process," in *IEEE MTT-S International Microwave Symp. Dig.*, vol. 2, pp. 963-966, 2003.

[2]. A. Chin, K. T. Chan, H. C. Huang, C. Chen, V. Liang, J. K. Chen, S. C. Chien, S. W. Sun, D. S. Duh, W. J. Lin, C. Zhu, M.-F. Li, S. P. McAlister and D. L. Kwong, "RF Passive Devices on Si with Excellent Performance Close to Ideal Devices Designed by Electro-Magnetic Simulation," in *International Electron Devices Meeting (IEDM) Tech. Dig.*, pp. 375-378, 2003.

[3]. C. H. Huang, K. T. Chan, C. Y. Chen, A. Chin, G. W. Huang, C. Tseng, V. Liang, J. K. Chen, and S. C. Chien, "The minimum noise figure and mechanism as scaling RF MOSFETs from 0.18 to 0.13 μm technology nodes," *IEEE RFIC Symp.*, pp. 373-376, 2003.

[4]. G. D. Vendelin, A. M. Pavio, and U. L. Rohde, "Microwave circuit design using linear and nonlinear techniques," John Wiley & Sons, p. 140, 1990 Edition.

[5]. P. R. Gray, P. J. Hurst, S. H. Lewis, and R. G. Meyer, "Analysis and design of analog integrated circuits", 4th edition, John Wiley & Sons, Chap. 11, pp. 773-783, 2001.

[6]. C. H. Chen and M. J. Deen, "A general Noise and S-parameter deembedding procedure for on-wafer high-frequency noise measurements of MOSFETs," *IEEE Trans. Microwave Theory Tech.*, vol. 49, pp. 1004-1005, 2001